

# Influence of Gamma Prime Evolution on the Creep Behaviour of SX Nickel Base Superalloys

Maurizio Maldini, Valentino Lupinc and Giuliano Angella

CNR –IENI, Via Cozzi 52 – I20125 Milano, Italy

maldini@ieni.cnr.it, lupinc@ieni.cnr.it, angella@ieni.cnr.it

**Key words:** creep, single crystal nickel base superalloy, raft microstructure

**Abstract.** The objective of this paper is to critically analyse the effect of the  $\gamma'$  morphology evolution on the creep strain rate behaviour in the temperature range 900 - 1100°C where rafts form in superalloys for single crystal turbine blade and vane applications. A close examination of the experimental results has shown different regimes of strain accumulation depending on the value of the applied stress and temperature. The experimental results have been rationalised in terms of the  $\gamma'$  shape evolution during creep.

## Introduction

The long and large tertiary stage, that dominates the creep curve shape of  $\gamma'$  reinforced nickel base superalloys for temperatures/stresses relevant for high temperature components, has been often modeled supposing a single strain softening mechanism is operative. For example the accelerating tertiary creep has been often described by a linear dependence of strain rate on strain[1-4]:

$$\dot{\epsilon} = \dot{\epsilon}^0 (1 + C\epsilon) \quad (1)$$

where  $\dot{\epsilon}$  and  $\epsilon$  respectively correspond to the instantaneous strain rate and the accumulated creep strain,  $\dot{\epsilon}^0$  represents the creep strain rate extrapolated to  $\epsilon = 0$ , and  $C$  is a parameter of proportionality between creep damage and the strain,  $W = C\epsilon$ . The relationship in Eq. 1 has been physically justified in [5] supposing the softening in nickel base superalloys is due to the accumulation of mobile dislocations that are proportional to the creep strain. Time softening, due to the ripening of the particles, is not considered in Eq. 1. Single crystal nickel base superalloys, with a large fraction of hardening cuboidal  $\gamma'$ , if creep tested under tensile load along  $\langle 001 \rangle$  crystalline direction at high temperature, can produce a lamellar or rafted  $\gamma/\gamma'$  pattern perpendicular to the loading axis. This  $\gamma'$  coalescence process can happen only at high temperatures, typically at  $T \geq 900^\circ\text{C}$  depending on the alloy, and very early, i.e. within the first 1-3% of creep life, for  $T > 1000^\circ\text{C}$ . In fact, for tests performed around  $900^\circ\text{C}$ , the cuboidal microstructure is generally present for a considerable part of the creep test: the raft development can start in correspondence of the minimum creep rate and ends well inside the tertiary creep [4] and consistently only a slight influence of the microstructure instability can appear on the creep behaviour at this temperature. Instead, at higher temperatures,  $1050\text{-}1100^\circ\text{C}$ , the cuboidal microstructure disappears soon, the cubic  $\gamma'$  develops into lamellae in the early primary creep, and the raft structure is present during almost the whole creep test. To extrapolate the creep behaviour at such experimental conditions from data obtained at lower temperatures, the microstructure instability must be taken into account, since the raft development can strongly influence the dislocation mobility when the dislocations cannot easily cut the long rafted  $\gamma'$ , particularly at low stress values typical of the creep tests performed at such high temperatures.

The purpose of the present paper – a synthesis partly drawn on previous publications [4, 6-9] - is to summarize the studies of the influence of the  $\gamma'$  morphology evolution on the creep strain rate in the  $900\text{-}1100^\circ\text{C}$  temperature range mostly important for single crystal components in high performance gas turbines. A better knowledge of the influence of the  $\gamma'$  morphology evolution on the creep curve is useful to improve methodologies able to predict service life of critical gas turbine components.

## Materials

The nominal compositions of the three Re containing superalloys, designed for gas turbine single crystal blades/vanes and considered in this paper, are shown in Table 1. The heat treatment and the experimental procedures are reported in [7,8] for alloy SMP 14 and in [4] for alloy TMS 75.

Table 1 Nominal compositions of SMP 14, TMS 75 and CMSX-4 superalloys (weight %).

Alloy	Cr	Co	Mo	W	Re	Ta	Al	Ti	Nb	Hf	Ni
SMP 14	4.8	8.1	1.0	7.6	3.9	7.2	5.4	-	1.4	-	Bal.
TMS 75	3.0	12.0	2.0	6.0	5.0	6.0	6.0	-	-	0.1	Bal.
CMSX-4	6.5	9.0	0.6	6.0	3.0	6.5	5.6	1.0	-	0.1	Bal.

## Microstructure, Creep and Correlation between Creep and Microstructure Evolution

**SMP 14 SX superalloy.** The rafts formation and their evolution, and their effect on the creep behaviour, have been studied on superalloy SMP 14 [10] - developed by CSIR, Pretoria RSA and supplied by Ross & Catherall Ltd Sheffield UK - at 900, 950, 1000 and 1050°C and with applied stresses among 425 and 135 MPa to produce times to rupture between 300 and 3000 h [7].

In Fig. 1 two examples of microstructure are shown: a micrograph of standard heat treatment cuboidal  $\gamma'$  microstructure and a longitudinal section of interrupted creep test specimen after 330 h at 1000°C/200 MPa, corresponding to about half of the creep life and a creep strain of 1.5%.

Fig. 2 is an example to show that Eq. 1 can well describe the rate of strain accumulation for almost the whole experimental tertiary creep. The plots of Figs 2 and 3c are equivalent, i.e. experimental points that show a linear relationship in a plot  $\dot{\epsilon}$  vs  $\epsilon$ , must also display a linear relationship in a plot  $\log \dot{\epsilon}$  vs time. The latter plot expands the initial portion of the creep curve, and it appears to be more convenient to observe possible time dependent effects occurring during the early creep strain. In fact, the juxtaposition of the same creep curves in Fig. 2 and in Fig. 3c reveals new unusual features hidden in the  $\dot{\epsilon}$  vs  $\epsilon$  plots. The experimental results show that, in addition to the strain softening damage described by Eq. 1, other microstructure dependent mechanisms influence the creep strain accumulation. In particular the analysis of Figs 3, combined with the microstructure observations of creep interrupted tests [9] showed that:

- stage A: In correspondence of the building up of the raft microstructure, the thickness of the horizontal  $\gamma$  channels significantly increases producing a reduction of the Orowan resistance of the dislocation mobility. Such microstructure evolution damage, added to the damage described by Eq.1, causes the fastest acceleration stage;
- stage B: after raft formation at high stress, the  $\gamma$  channels continue to grow moderately. During the stage B, where most of the creep strain is accumulated in a relatively short time, the strain acceleration can be described by Eq. 1;

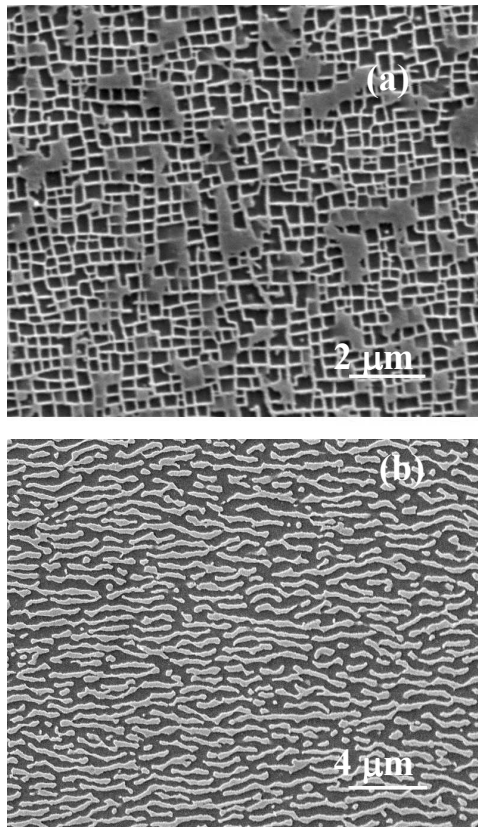


Fig. 1 – SMP 14 SEM micrographs of: a) material after standard heat treatment and b) longitudinal section of interrupted creep tested specimen after 330 h at 1000°C/200 MPa

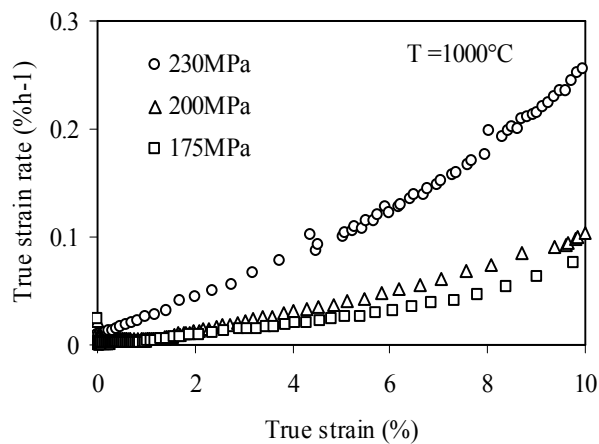


Fig. 2 – SMP 14 creep rate vs. strain at 1000°C.

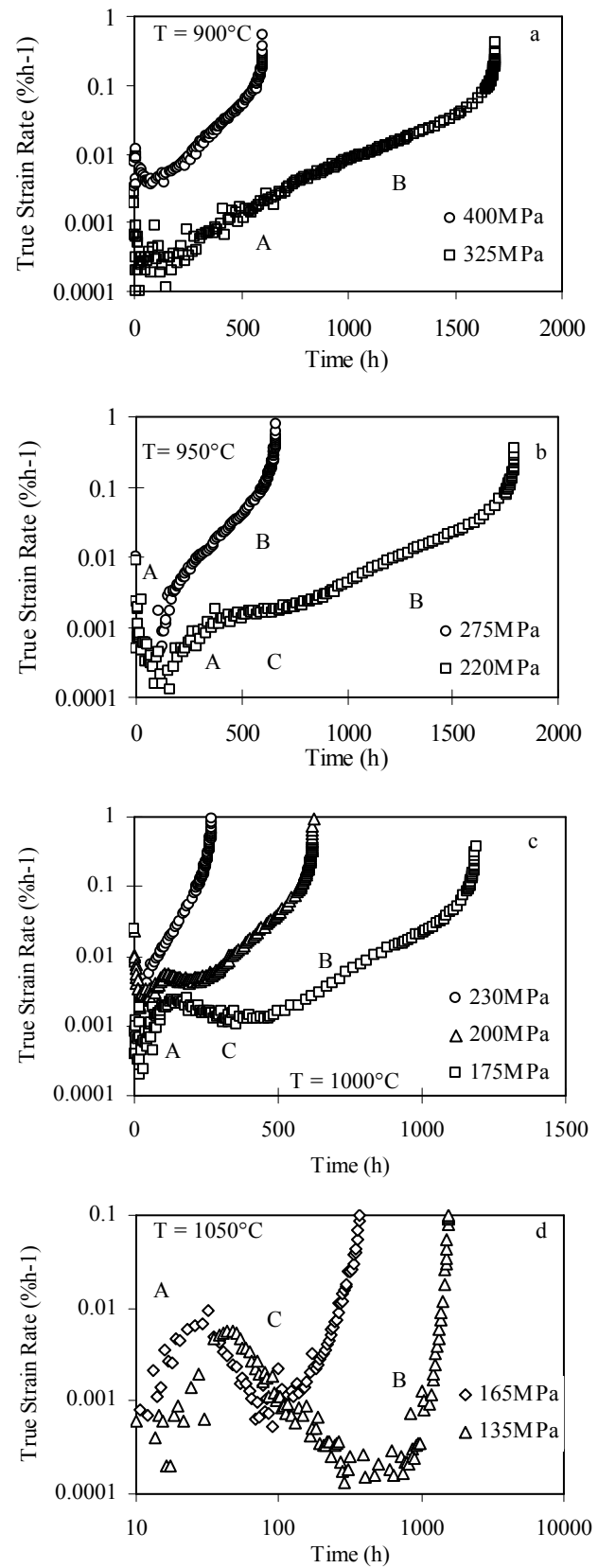


Fig. 3 - SMP 14 creep plots  $\log(d\epsilon/dt)$  vs time in tests a) 900°C, b) 950°C and c) 1000°C, and  $\log(d\epsilon/dt)$  vs  $\log$  time in tests d) at 1050°C.

- stage C: after raft formation at low stress, a further regime of strain accumulation, stage C, appears between stages A and B; it can be due to two concurring mechanisms, i.e.:

i) The increment of dislocation density in the  $\gamma/\gamma'$  interface relax the misfit stresses, reducing the local stress in the  $\gamma$  channels and making more difficult the movement of dislocations. This process can partially explain the rapid decrement of the strain rate after the raft development in the tests at the highest temperatures.

ii) For material with completely developed rafted structure, the  $\gamma$  phase cannot easily flow around the  $\gamma'$  phase because the  $\gamma$  lamellae are essentially unconnected. Supposing the dislocation activity is mainly restricted into the  $\gamma$  phase, during creep the  $\gamma$  phase can plastically deform, while the  $\gamma'$  phase basically can deform only elastically. Essentially the material can be considered as a metal matrix composite with the two phases deforming simultaneously. During creep, the stress is off-loaded from the "soft" matrix regions ( $\gamma$ ), while the stress in the "hard" reinforcing zones ( $\gamma'$ ) is amplified [9]. In the rafted material, the decreasing of the stage C slope, becoming negative at applied stress values below 200 MPa, reflects the reducing of the local stress in the  $\gamma$  channel. In principle the creep rate should progressively decrease, with increasing creep strain, as the local stress in the  $\gamma$  phase approaches the Orowan and solid solution resistance.

Actually the reduction of the creep strain rate with the strain ends when, in absence of some other damage mechanisms, a recovery process prevents a further stress redistribution between the two phases. The simplest recovery process consists in the cutting of the  $\gamma'$  phase by the interface dislocations; this recovery process could be operative after the accumulation of plastic strain in the  $\gamma$  phase has built up a sufficient internal stress, that in conjunction with the external applied stress, allows the cutting of the  $\gamma'$  phase.

**TMS 75 SX superalloy.** The raft formation and evolution, and their effect on the creep behaviour have been studied on TMS75 superalloy developed by NIMS Tsukuba Japan, with the help of a large number of interrupted creep tests. The results have been presented in [6]. No qualitative differences can be observed neither between the experimental creep curves of this alloy and on SMP 14 at 900°C nor between this alloy at 1100°C and SMP 14 at 1050°C, respectively. In particular both the alloys show the two different rates of damage accumulation, stage A and stage B, at 900°C, Figs 4a and 3a .

In [9] it is shown that, at 900°C, the raft development occurs in SMP 14 in correspondence of the first tertiary creep (stage A in Fig 3a) and the rafts are completely developed at the beginning of the stage B. Similar conclusions are drawn in [6] for the TMS75. In TMS 75 at 1100°C and in SMP 14 at 1050°C, after the initial creep accelerating stage a clear decelerating stage appears. The combination of hardening and softening processes, during stages C and B, respectively, produces a clearly apparent minimum creep rate, Figs 4b and 3d.

A large number of interrupted creep tests of TMS 75 at 900°C/392 MPa and 1100°C/137 MPa permitted detailed microstructure studies that lead to graphs of gamma channels average thickness growth during creep, shown in Figs 5a and b, that confirmed the microstructure evolution hypotheses [6].

**CMSX-4 superalloy.** A similar phenomenon of  $\gamma'$  formation and evolution influence on creep behaviour appears also in two of the creep curves shown in Fig. 6, i.e. at 950°C under 220 and 155 MPa [11], confirming that this kind of effects is detected quite often.

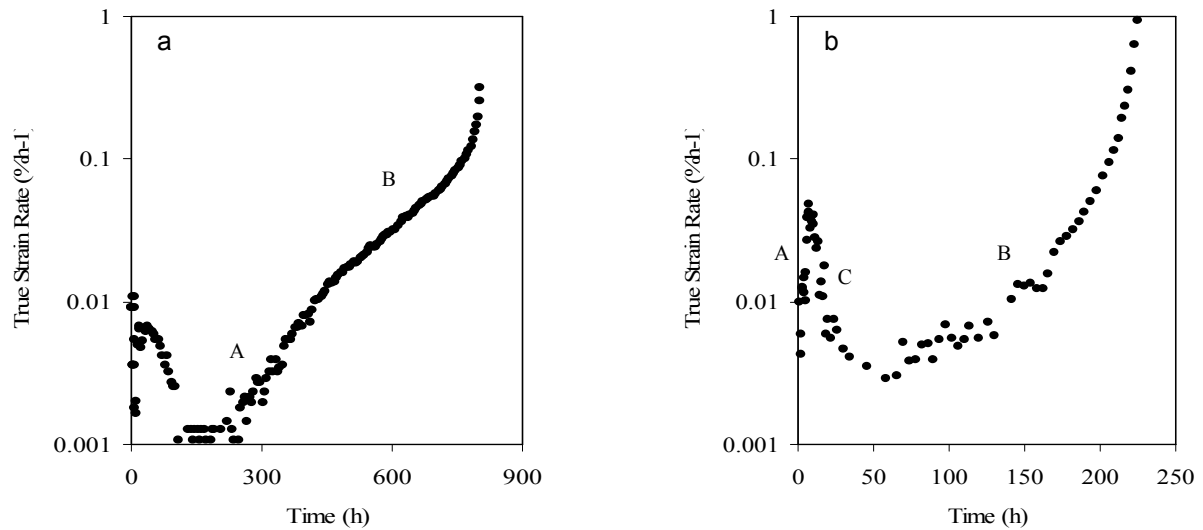


Fig. 4 – TMS 75 experimental creep curves at: a) 900°C/392 MPa and b) 1100°C/137 MPa.

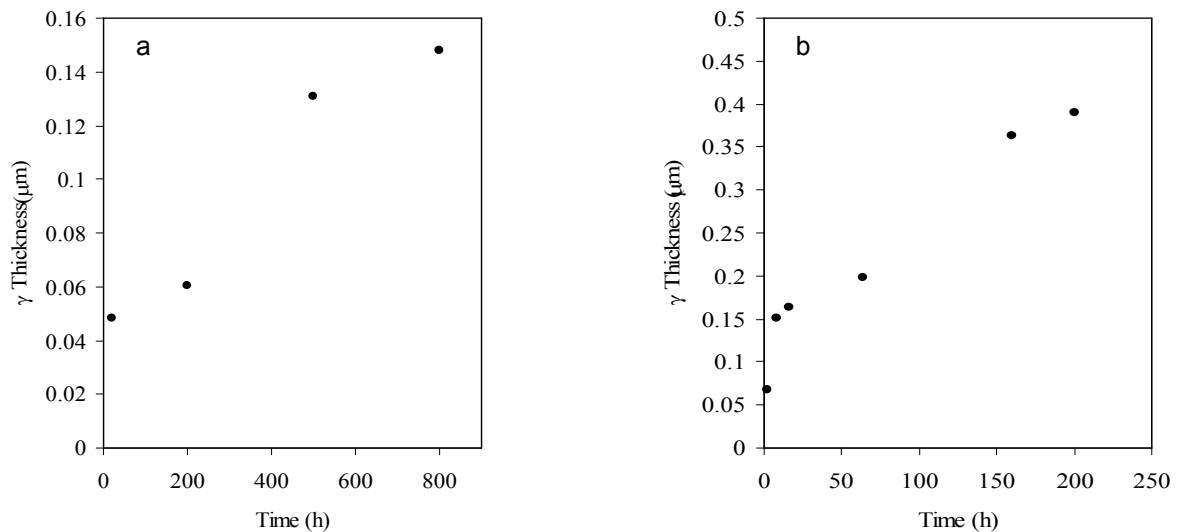


Fig. 5 TMS 75 evolution of  $\gamma$  channel width during creep at: a) 900°C/392 MPa, b) 1100°C/137 MPa

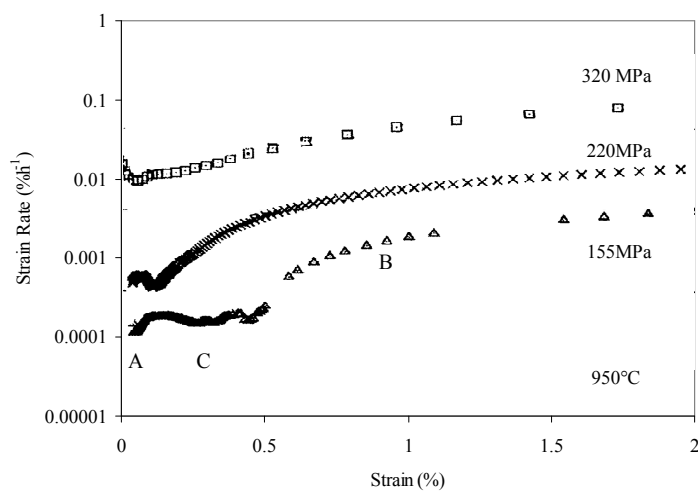


Fig. 6 – CMSX-4 experimental creep curves at 950°C/320, 220 and 155 MPa.

## Conclusions

The analysis of the experimental creep curves of the SMP 14 and TMS 75 alloys in the 135-425 MPa/900-1050°C testing range has shown:

- The tertiary creep dominates the creep curves.
- In the explored stress/temperature field, a rafted microstructure is developed during creep.
- At the highest explored temperatures the raft development is very rapid and takes only a few percent of the creep life, while at 900°C rafts are developed only in late tertiary creep.

During tertiary creep, different stages can be distinguished:

- a strongly creep accelerating stage, that occurs during the raft development;
- a stage that produces a reduction of the strain rate for the highest temperatures/lowest stresses explored: this stage has been attributed to a redistribution of the local stresses between the  $\gamma$  and  $\gamma'$  phases and it disappears in the highest stresses tests;
- a further stage where the strain accelerates again, with the strain rate following a linear strain softening relationship in the 900-1000°C interval.
- The fastest and shortest final creep accelerating stage, leading to fracture.

Similar phenomena as synthesized above seem to appear also in CMSX-4 alloy at 950°C in the 150 – 220 MPa stress range.

## References

- [1] B. Dyson and M McLean: Acta Metall., 31 (1983), p. 17.
- [2] M. Maldini and V. Lupinc: Materials at High Temperatures, 14 (1997), p. 47.
- [3] M. Maldini and V. Lupinc: Scripta Met., 22 (1988), p. 1737.
- [4] M. Maldini et al.: Scripta Mater., 43 (2000), p. 637.
- [5] B.F. Dyson: Revue Phys.Appl., 23 (1988), p. 605.
- [6] M. Maldini et al.: International Journal of Materials Processing Technology, 117 (2001), p. .
- [7] M. Maldini et al.: Proc. Materials for Advanced Power Engineering 2002, ed. by J. Lecomte-Beckers et al., Forschungszentrum Jülich, Jülich, Germany, 2002, Part I, p. 167.
- [8] M. Maldini et al.: Kovové Materiály, 42 (2004), p. 21.
- [9] M. Maldini et al.: Proc. Advanced Materials and Processes for Gas Turbines, ed. by G. Fuchs et al., TMS, Warrendale, PA, USA (2003) p. 161.
- [10] N. Gravill et al.: Proc. Materials for Advanced Power Engineering 1998, ed. by J. Lecomte-Beckers et al., Forschungszentrum Jülich, Jülich, Germany, 1998, Part II, p. 1025.
- [11] B. Fedelich et al.: Mat. Sci. Engng A, 510-511 (2009), p. 273.